

000 001 002 003 004 005 006 007 008 009 010 MEASURING SPARSE AUTOENCODER FEATURE SENSITIVITY

005 **Anonymous authors**

006 Paper under double-blind review

009 ABSTRACT

011 Sparse Autoencoder (SAE) features have become essential tools for mechanistic
 012 interpretability research. SAE features are typically characterized by examining
 013 their activating examples, which are often “monosemantic” and align with human
 014 interpretable concepts. However, these examples don’t reveal *feature sensitivity*:
 015 how reliably a feature activates on texts similar to its activating examples. In this
 016 work, we develop a scalable method to evaluate feature sensitivity. Our approach
 017 avoids the need to generate natural language descriptions for features; instead
 018 we use language models to generate text with the same semantic properties as a
 019 feature’s activating examples. We then test whether the feature activates on these
 020 generated texts. We demonstrate that sensitivity measures a new facet of feature
 021 quality and find that many interpretable features have poor sensitivity. Human
 022 evaluation confirms that when features fail to activate on our generated text, that
 023 text genuinely resembles the original activating examples. Lastly, we study feature
 024 sensitivity at the SAE level and observe that average feature sensitivity declines
 025 with increasing SAE width across 7 SAE variants. Our work establishes feature
 026 sensitivity as a new dimension for evaluating both individual features and SAE
 027 architectures.

028 1 INTRODUCTION

030 Sparse Autoencoders (SAEs) have emerged as a powerful technique to identify meaningful directions
 031 in language model activation spaces (Cunningham et al., 2023; Templeton et al., 2024). These learned
 032 directions, or SAE features, have proven to be valuable for mechanistic interpretability. Use cases include:
 033 surfacing surprising information present in model activations (Templeton et al., 2024; Ferrando et al., 2025), controlling model behavior via activation steering (Durmus et al., 2024;
 034 Nanda et al., 2025), identifying computational circuits within models (Ameisen et al., 2025; Marks et al., 2025a; Lindsey et al., 2025), and more open-ended exploration of training data (Marks et al., 2025b) or other datasets (Movva et al., 2025; Jiang et al., 2025).

038 A key step in almost all SAE applications is to first characterize each SAE feature. This is commonly done by examining example inputs that activate each feature. These activating examples are often cohesive and correspond to human-interpretable concepts (Cunningham et al., 2023; Templeton et al., 2024), e.g., “harmful requests”. However, only examining a feature’s activating examples tells us what a feature does but not what it fails to do. We might hope that a harmful request feature activates on all harmful requests, but we cannot determine this by just examining activating text. Additionally, we need to evaluate *feature sensitivity*: the probability that a feature activates on texts similar to its activating examples.

046 Ideally, features would have high sensitivity—consistently activating on all relevant inputs rather than arbitrary subsets. Understanding a feature’s sensitivity is crucial for scoping what we can learn from the feature. If a harmful request feature has high sensitivity and activates on all harmful requests, understanding its role can reveal how the model generally processes any harmful input. If, instead, the harmful request feature has poor sensitivity, we are mainly gaining narrower insights into how the model handles the specific input that activates the feature.

052 In this work, we use a generation-based approach to evaluate feature sensitivity at scale. As illustrated in Figure 1, we use language models to generate text with the same semantic properties as a feature’s activating examples. We then test whether the feature activates on these generated texts.

108 2.2 SAE EVALUATION
109110 Earlier work primarily evaluated SAEs by their reconstruction error and the interpretability of individual
111 features (Bricken et al., 2023; Templeton et al., 2024).
112113 Although increasing SAE width improves both reconstruction quality and feature interpretability
114 (Karvonen et al., 2025), a growing body of research investigates problems that arise when scaling
115 SAEs, including feature splitting (Bricken et al., 2023), feature absorption (Chanin et al., 2024), and
116 feature composition (Leask et al., 2025). These results highlight that only optimizing for sparsity
117 and reconstruction may not yield natural features.
118119 Another line of work evaluates SAE latents by their utility for downstream tasks: sparse probing
120 (Gao et al., 2024), spurious correlation removal (Marks et al., 2025a), disentangling model representations
121 (Huang et al., 2024), and unlearning (Farrell et al., 2024). Karvonen et al. (2025) introduce
122 SAEBench, a benchmark that aggregates many of these evaluation approaches, along with standard
123 automated interpretability and reconstruction metrics.
124125 2.3 AUTOMATED INTERPRETABILITY
126127 The standard auto-interpretability pipeline involves collecting activating text examples for a feature,
128 prompting an LLM to generate natural language descriptions from these examples, and validating
129 these descriptions by testing whether they enable another LLM to predict activations on new text.
130 Bills et al. (2023) first proposed this approach for neurons, and it has since become standard for both
131 neuron explanations (Choi et al., 2024) and SAE explanations (Paulo et al., 2024; Templeton et al.,
132 2024; Karvonen et al., 2025).
133134 A complementary approach evaluates explanation quality by testing whether explanations can gen-
135 erate new activating inputs. This approach has been used to evaluate both neuron explanations
136 (Huang et al., 2023) and SAE feature explanations (Juang et al., 2024). Other work uses input gen-
137 eration to help interpretability agents test hypotheses about component activation (Shaham et al.,
138 2025). Similar generation-based evaluation approaches have been applied beyond language models
139 to explanations of vision neurons and other components (Singh et al., 2023; Kopf et al., 2024).
140

3 EVALUATING FEATURE SENSITIVITY

141 3.1 EVALUATING FEATURE SENSITIVITY INDEPENDENT OF EXPLANATION
142143 Previous work on sensitivity typically relies on some (typically natural language) description to
144 identify test inputs (Turner et al., 2024; Juang et al., 2024). Such methods evaluate sensitivity as a
145 function of both the model component and the corresponding explanation. When studying neurons,
146 which are a part of the model itself, such approaches cleanly evaluate how well an explanation
147 describes a neuron’s activating inputs. However, SAE features present a more complex challenge.
148149 Unlike neurons, SAE features are learned approximations of a model rather than intrinsic model
150 components. Much prior work has identified and addressed limitations in feature quality arising
151 from SAE training (Chanin et al., 2024; Leask et al., 2025; Marks et al., 2024; Bussmann et al.,
152 2025). Because SAE features and generated feature descriptions are imperfect, evaluating feature
153 sensitivity with explanations may struggle to distinguish between an inaccurate description of a
154 feature and a feature failing to activate on relevant inputs.
155156 We avoid this ambiguity by evaluating feature sensitivity without generating an explanation. As
157 shown in Figure 1, we prompt language models with a feature’s activating text examples to generate
158 similar text samples, then measure how often the feature activates on these new texts. For a feature
159 to achieve high sensitivity, it must consistently activate on novel inputs that human judges find indis-
160 tinguishable from the original activating examples. This approach effectively measures sensitivity
161 as if we had a perfect explanation—one precise enough to generate indistinguishable examples but
nothing broader.

162	Feat ID: 297594	Desc: the word 'problems' and related concepts indicating issues or challenges	Freq: 3.33e-05	Sensitivity: 60.00%	Interp Score: 100.00%
Activating Text Examples					
163					
164	8.75 of a trendy Melbourne art gallery, has her own problems – chasing down a delinquent				
165	7.34 to attempts at calibration. ↪ ↪ Of course, our problems are not likely to clear up so one may				
166	12.62 him, that's only the start of their problems . ↪ ↪ In this third Alex Caine book, sequel				
167	6.78 mnir becomes queen of a land with as many problems as the one she fled. Her long-lived				
168					
169	Feat ID: 593453	Desc: the substring 'math' in mathematical notation and equations	Freq: 2.22e-05	Sensitivity: 0.00%	Interp Score: 92.86%
170	Generated Text				
171	6.97 facing constant delays, she explained her problems quietly but with visible frustration at the				
172	0.00 discussing legislative issues, where the problems often are complex and intertwined with				
173	8.12 Nina realized that understanding his problems required stepping into his perspective; that				
174	0.00 explaining the malfunction during the software demo, he hoped the technical problem would				

Figure 2: **Interpretable features with moderate and low sensitivity.** Feature activations are shown on top activating texts (left) and on LLM-generated texts from our evaluation (right). Generated text is formatted to indicate tokens expected to activate the feature. These are highlighted when the feature remains inactive.

3.2 METHOD DETAILS

Our sensitivity evaluation approach consists of four steps: (1) collect activating text examples for each feature, (2) generate new texts similar to these examples using an LLM, (3) evaluate if the feature is active on these new texts, and (4) compute sensitivity score as the fraction of new generated texts which successfully cause the feature to activate. In the paragraphs below, we provide additional details for the first two steps. Figure 2 shows examples of text generated by our evaluation.

Collecting Activating Text: We sample 2 million tokens of candidate texts from large text corpora. The corpus is OpenWebText (Gokaslan et al., 2019) for SAE Bench evaluations and the Pile-uncopyrighted subset (Gao et al., 2020) for GemmaScope evaluations. We evaluate feature activation on sequences of 128 tokens, following the example collection methodology used in (Karvonen et al., 2025). When a feature activates, we extract the activating example by including 10 tokens preceding and 10 tokens following the activating token. For each feature, we collect 15 activating text examples: 10 top activating examples and 5 importance-weighted samples by activation magnitude.

Generating New Texts: We provide activating text examples when prompting an LLM. We do *not* use any natural language descriptions of the feature in the prompt. In preliminary experiments, adding automated feature descriptions reduced the probability that generated text would activate the feature. From inspecting samples, we believe this is due to automated descriptions that are sometimes overly general and imprecise. For each feature, we use a single query to generate 10 new text samples. We found that a single query produced more diverse outputs than multiple independent queries. The full prompts are included in Appendix A. We use GPT-4.1-mini (OpenAI et al., 2024) for the generation step. We found that it produced text comparable to GPT-4.1, while GPT-4.1-nano struggled to complete the generation task.

Method Assumptions: Our method relies on several key assumptions. First, we require that our collected examples adequately capture each feature’s behavior, which we ensure by following standard approaches for collecting activating examples and filtering out features that fail to activate on truncated text. Details of filtering are described in Section 3.3. Second, we assume that generated texts share whatever semantic property triggers feature activation, which we validate through human evaluation in Section 5.1. Third, we assume generated samples are sufficiently novel and diverse to serve as valid tests of sensitivity, which we verify in Section 5.2.

3.3 FILTERING SAE FEATURES

We limit our study to SAE features that meet two criteria. First, we only evaluate features for which we can collect at least 15 activating text samples from 2 million tokens, which filters out rare features. Second, we found that many features fail to activate on their own truncated examples, so we filter for features where at least 90% of the shortened text snippets still activate the feature. This

filtering may bias our analysis toward simpler features, but it ensures that features failing to activate on generated text genuinely reflect poor sensitivity, rather than an artifact of sample text truncation. The fraction of filtered features increases substantially with SAE width. For smaller SAEBench SAEs (width 4k to 65k), we exclude 35% of features on average. For GemmaScope SAEs, this ranges from 51% for 65K width SAEs to 79% for 1M width SAEs. Detailed filtering statistics and results with different cutoffs are shown in Appendix B.

4 FEATURE SENSITIVITY CAPTURES NOVEL ASPECTS OF FEATURE BEHAVIOR

We begin by examining the relationship between our feature sensitivity metric and standard SAE feature evaluation metrics. For this, we study the canonical (width 1M, sparsity 107) GemmaScope (Lieberum et al., 2024) SAE for the layer 12 residual stream of Gemma 2 2B (Team et al., 2024). We sampled 10,000 SAE features. After filtering per Section 3.3, 2,061 remained for analysis.

We show the distribution of sensitivities across all features in Figure 3a. Most features score well on sensitivity, but the features span all sensitivity scores, showing meaningful variation in feature quality when measured via sensitivity.

Next, we examine three key feature properties for comparison. First, we look at feature interpretability, which we measure using the automated interpretability evaluation of (Karvonen et al., 2025). Second, we examine feature frequency, which is how often features have nonzero activation. Third, we compute the maximum decoder cosine similarity between a feature’s decoder vector and all other feature decoder vectors. High similarity may reflect undesirable feature composition or entanglement (Bussmann et al., 2025).

The three scatter plots of feature sensitivity and each property (Figures 3b, 3c, and 3d) confirm that feature sensitivity is distinct from existing other metrics. We find weak correlations of sensitivity with frequency ($\rho = -0.06$) and decoder cosine similarity ($\rho = 0.06$), and a stronger correlation between sensitivity and interpretability score ($\rho = 0.24$). The overall weak correlations with existing metrics are encouraging—they suggest that sensitivity captures a novel and complementary dimension of feature quality rather than simply replicating existing evaluations.

Although feature interpretability and feature sensitivity are correlated, they often disagree. When examining features with high sensitivity but low auto-interpretability scores, we find this mainly reflects noise in the automated evaluation—these features appear qualitatively interpretable upon inspection. More importantly, *we find many interpretable features exhibit poor sensitivity*. Among 1347 features with auto-interpretability scores ≥ 0.9 , 82 have sensitivity ≤ 0.5 , and 23 have sensitivity ≤ 0.2 . Figure 2 shows examples of interpretable features with moderate and low sensitivity, with additional examples in Appendix G. Spot checking these features shows that our evaluation-generated text resembles activating text but fails to activate the feature, suggesting that our method has indeed found interpretable features that have poor sensitivity. In the next section, we validate this rigorously via human evaluation.

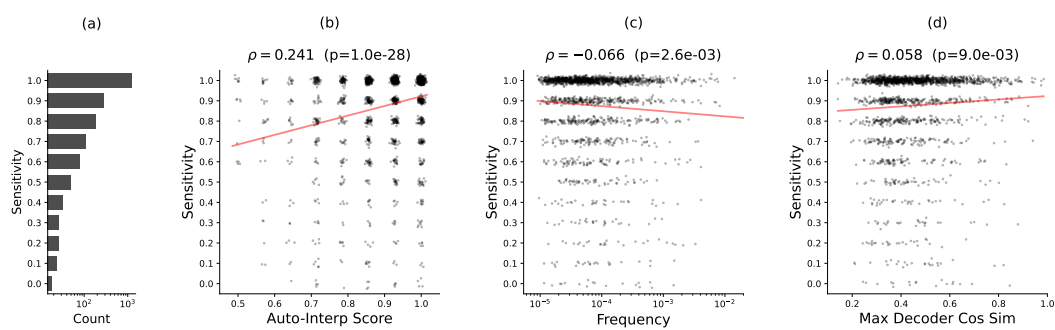


Figure 3: **GemmaScope SAE feature sensitivity distributions.** The distribution of feature sensitivity and scatter plots showing joint distributions of sensitivity with auto-interpretability, frequency, and maximum decoder cosine similarity. Sensitivity scores in scatter plots are plotted with y-jitter for visualization. Correlation coefficients and p-values are shown at the top of each scatter plot.

270 5 VERIFYING THE AUTOMATED SENSITIVITY EVALUATION

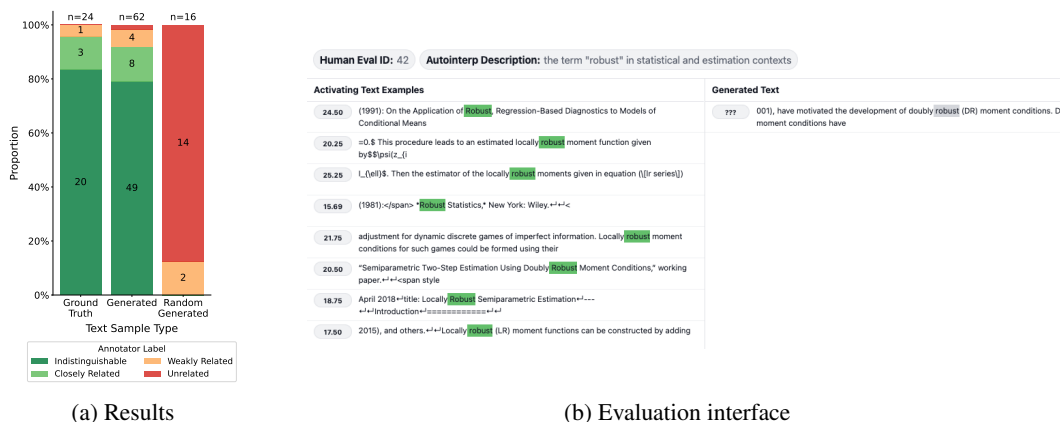
272 We validate that our automated sensitivity evaluation is reliable through two analyses: (1) human
 273 evaluation of sample similarity and (2) automated evaluations of sample novelty and diversity.
 274

275 5.1 BLINDED HUMAN EVALUATION

277 The goal of the human evaluation is to check if human annotators agree that the LLM generations are
 278 indeed consistent with the feature concept, and therefore appropriate for scoring feature sensitivity.
 279

280 Human annotators judged 102 examples in total. Each example consists of several activating text
 281 examples for a feature along with one new text sample. The new text can be one of three categories:
 282 another activating text example for the feature (20%, positive control), a generated text for a random
 283 other feature (20%, negative control), or a text generated by our method that failed to activate the
 284 feature (60%). The category is not revealed to the human annotator. The human annotator is then
 285 asked to classify whether the new text is “indistinguishable”, “closely related”, “weakly related”, or
 286 “unrelated” to the provided activating text examples. A sample dashboard for the human evaluation
 287 is shown in Figure 4b. We only include features with high auto-interpretability (≥ 0.9). This allows
 288 the study to focus on verifying cases where we might be most skeptical of low sensitivity results a
 289 priori. Additionally, interpretable features are easier for human annotators to assess.

290 Results are shown in Figure 4a. *Generated text achieves relevance ratings nearly matching ground*
 291 *truth, confirming that low sensitivity evaluations reflect poor sensitivity rather than poor generation.*
 292 Human annotators rate our method’s generated texts ($n = 62$) nearly as relevant to the feature as
 293 the ground truth texts: 79% of generated texts are rated “indistinguishable”, compared to 83% of
 294 ground truth activating texts. Only one out of 62 generated texts is rated “unrelated”. Additionally,
 295 annotators correctly scored controls: positive control texts ($n = 24$) are rated “indistinguishable” or
 296 “closely related” 96% of the time, while all negative control texts ($n = 16$) are rated “unrelated” or
 297 “weakly related”.



312 **Figure 4: Human evaluation validates our method.** (a) Human evaluation of 102 text samples
 313 across three conditions: true activating text examples (positive control), text generated for random
 314 features (negative control), and text generated by our evaluation that failed to activate features.
 315 (b) The interface shows feature activating examples alongside generated text for evaluation, with
 316 annotators rating similarity.

317 5.2 SAMPLE NOVELTY AND DIVERSITY

318 The goal of this analysis is to check that (1) our generated texts were not copying the activating
 319 examples, i.e., the diversity between each generated text and the top-activating texts is sufficiently
 320 high, and (2) our generated texts covered a wide range of feature expression, proxied by checking
 321 that the diversity between generated texts is sufficiently high.

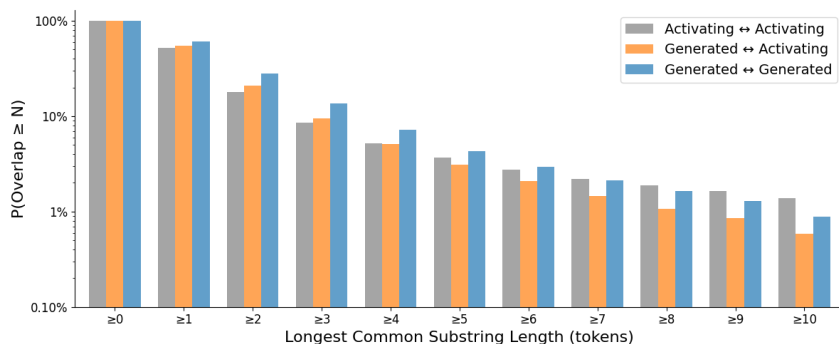


Figure 5: **Text diversity validation.** Probability that the longest common substring length is $\geq N$ tokens. We compare: two activating text examples for the same feature (gray), one generated text and one activating text example for the same feature (orange), and two generated text samples for the same feature (blue).

We assess text diversity by measuring the longest common substring length across three comparisons: (1) between generated text with activating examples to evaluate copying, (2) between pairs of activating examples to establish baseline overlap levels, and (3) between pairs of generated texts to assess diversity within our generations. Also note that we checked for longest substring match ending on the activating tokens, since only tokens before the activating part contribute to the activation.

Figure 5 shows the complementary cumulative distribution function (CCDF) for longest common substring lengths. Each bar shows the fraction of text pairs with overlap $\geq N$ tokens: gray bars show overlap between activating examples (baseline), orange bars show overlap between generated and activating texts (testing for copying), and blue bars show overlap between generated texts (testing for diversity).

The first reassuring observation is that a generated text and an activating text example are less likely to have a long overlap than two activating examples (3.1% v.s. 3.7% at ≥ 5 tokens). On the other hand, a generated text and an activating text example are more likely to contain a short overlap than two activating examples (20.8% v.s. 18.0% at ≥ 2 tokens). This indicates that our generated texts occasionally use short verbatim sequences from the examples but avoid copying long passages.

Two generated texts are slightly more likely to have overlap than the baseline between activating examples, with 27.9% probability of ≥ 2 token overlap and 4.3% at ≥ 5 tokens. This reveals that pairs of generations show somewhat lower diversity, though the difference is modest. This overlap pattern likely reflects LLM preferences for common word choices and short phrases rather than wholesale copying. While generation diversity can be improved, there are no pathological issues with extended substring duplication.

6 EVALUATING FEATURE SENSITIVITY ACROSS SAEs

Having explored the sensitivity of features within a single SAE and having confirmed that our evaluation method is reliable, we now turn to evaluating the average feature sensitivity across different SAE sizes and architectures.

6.1 RESULTS ON LARGE GEMMASCOPE SAEs

The GemmaScope suite of twenty nine JumpReLU SAEs range in size from 65K to 1M features and range in sparsity from 20 to 200 (Lieberum et al., 2024). These SAEs are trained to reconstruct the layer 12 residual stream of Gemma 2-2B (Team et al., 2024). For each SAE in GemmaScope, we collect activating texts for 2500 features, then apply the filtering criteria described in Section 3.2 and Appendix B before computing sensitivity.

Figure 6 shows the effect of dictionary width and sparsity on feature sensitivity. At a fixed dictionary size, sensitivity increases as sparsity increases. Strikingly, as SAE width increases, average feature

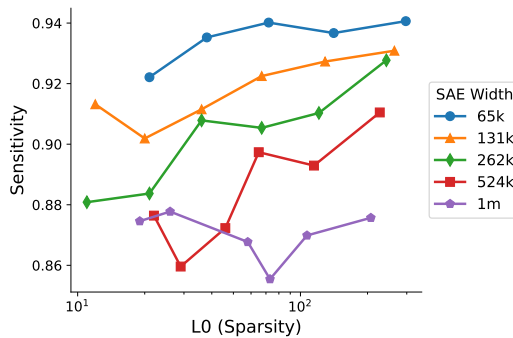


Figure 6: **Average Feature Sensitivity of GemmaScope SAEs.** For each dictionary size, we plot the feature sensitivity of SAEs trained at that size at different sparsities. Wider SAEs have worse average feature sensitivity. We also see that feature sensitivity is slightly increasing with sparsity.

sensitivity decreases. Concretely, 65K width SAEs have average feature sensitivities ranging from 0.92 to 0.94, while 1M width SAEs have feature sensitivities ranging from 0.85 to 0.87. Additionally we find that at a fixed width, SAEs with high L0 - more active features - have higher average feature sensitivity. In Appendix E we show that these two trends hold after controlling for feature frequency.

6.2 RESULTS ON DIVERSE SAE ARCHITECTURES

Having found these scaling trends on GemmaScope JumpReLU models, we next test whether they generalize across different model families and SAE architectures. We evaluate SAEs from the SAEBench collection (Karvonen et al., 2025), which includes 7 different SAE architectures trained on both Pythia-160M (Biderman et al., 2023) and Gemma-2-2B (Team et al., 2024) models. While these SAEs are much smaller in scale than GemmaScope, they allow us to validate our findings across SAE variants and model architectures. For each SAE studied here, we collect activating text for 1000 features, then filter as before.

We show the relationship between sparsity and sensitivity on the largest SAEs in this suite (65k width) in Figure 7. While the results are noisier due to smaller sample sizes, we see a general trend of sensitivity increasing with sparsity across model and SAE variants. While noise prevents us from making strong claims about sensitivity differences between each of the SAE architectures, vanilla ReLU SAEs consistently show low sensitivity, performing worst on Gemma-2-2B and among the worst variants on Pythia-160M.

Next, we examine how dictionary size affects sensitivity across architectures. To control for sparsity, we select SAEs with L0 closest to 80 (exactly 80 for top-K SAEs, closest available for other variants). The results in Figure 8 confirm that wider SAEs consistently show worse sensitivity across

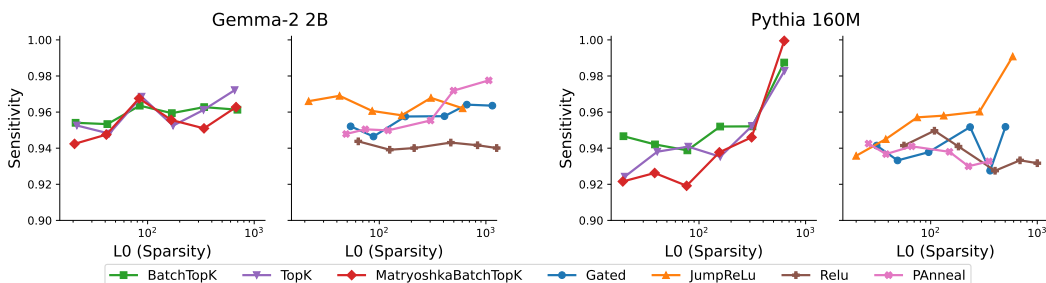


Figure 7: **Average Sensitivity vs. Sparsity for Gemma-2-2b and Pythia-160m SAEs** This plot shows the average sensitivity of different Sparse Autoencoder (SAE) types plotted against their sparsity. We use the widest 65k width SAEs for all architectures. Each line represents a different SAE architecture.

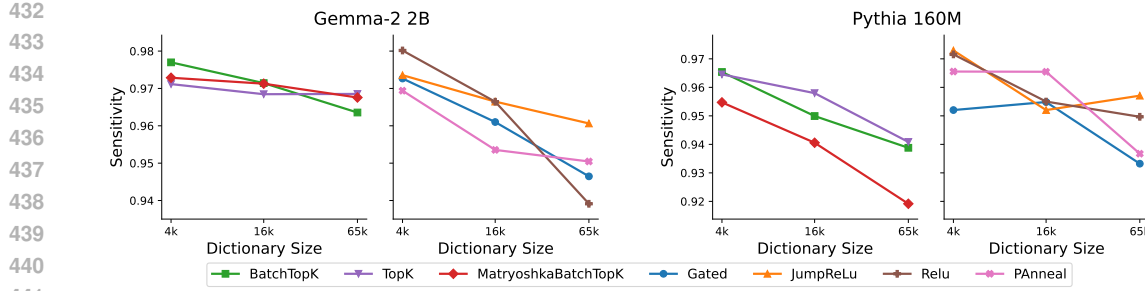


Figure 8: **Average Sensitivity vs. Dictionary Size for Gemma-2-2b and Pythia-160m SAEs** This plot shows the average sensitivity of different Sparse Autoencoder (SAE) types plotted against their dictionary size. We select SAEs with L0 closest to 80 (exactly 80 for top-K SAEs, closest available for other variants). Each line represents a different SAE architecture.

all tested architectures. Notably, *Matryoshka SAEs also exhibit negative scaling with sensitivity*, despite being specifically designed to address scaling challenges in SAEs (Bussmann et al., 2025).

7 DISCUSSION AND CONCLUSION

We developed a scalable pipeline that generates texts similar to SAE feature activating examples. We validate through human evaluation that these generated texts are genuinely similar—humans judge them as indistinguishable from actual activating examples. We use this pipeline to evaluate individual features and average sensitivity of features in an SAE. At the feature level, we found that many interpretable features have poor sensitivity, broadening our notion of what makes a high-quality SAE feature. At the SAE level, we found that average feature sensitivity consistently decreases as SAE width increases, identifying a new challenge for scaling SAEs. Taken together, our work helps develop feature sensitivity as a new axis to evaluate both individual features and SAE variants.

7.1 LIMITATIONS AND FUTURE WORK

Beyond evaluation, our pipeline opens new directions for exploratory analysis. Studying feature activations on text generated by our pipeline could enable more fine-grained studies of the boundaries separating activating from non-activating inputs for a given feature. This approach could also enable the study of groups of features that may collectively represent specific concepts with high sensitivity. Additionally, our pipeline and sensitivity evaluation can be applied to any model component that activates on input text. Future research could examine sensitivity in thresholded neurons, transcoders (Dunefsky et al., 2024), and cross-layer transcoders (Ameisen et al., 2025).

Our evaluation was limited to frequently occurring features (15+ times in 2M tokens), which biases our analysis toward common features and misses potentially important rare features. We filter for features that remain active when truncated activating text is used, potentially biasing toward simpler features that don’t depend on longer contexts. Future work can directly scale up this evaluation by studying less frequent features and using longer text snippets. Additionally, we don’t meaningfully incorporate information about the magnitude of feature activation in each passage. We would be excited by future work that incorporates activation strength into studies of SAE features, either in the context of sensitivity or broader evaluation.

486 REFERENCES AND REPRODUCIBILITY
487488 We have uploaded our code anonymously as supplementary material for the review process at
489 <https://anonymous.4open.science/r/sae-sensitivity-8247>. For the camera-ready version,
490 we will release it publicly on GitHub. We use publicly available SAEs from SAEBench (Karvonen
491 et al., 2025) and GemmaScope (Lieberum et al., 2024), and publicly available data from OpenWeb-
492 Text (Gokaslan et al., 2019) and the Pile (Gao et al., 2020). Implementation details are provided in
493 Section 3.2, with evaluation prompts in Appendix A.494
495 ETHICS STATEMENT
496497 Our work evaluates interpretability methods and does not directly enable new capabilities or appli-
498 cations. We recognize that improved understanding of neural networks could have dual-use impli-
499 cations, potentially aiding both safety research and capabilities development. Our human evaluation
500 was conducted by the authors themselves, avoiding concerns regarding external participants. All
501 experiments used publicly available models and datasets.502
503 USE OF LARGE LANGUAGE MODELS
504505 We used Claude Code and ChatGPT as general-purpose tools to assist with implementing experi-
506 ment code, generating plots, formatting the paper, and revising text. All LLM outputs were carefully
507 verified and checked by the authors. The research idea, experimental design, and conclusions were
508 developed by the authors without LLM assistance. The authors take full responsibility for all content
509 in this work.510
511
512
513
514
515
516
517
518
519
520
521
522
523
524
525
526
527
528
529
530
531
532
533
534
535
536
537
538
539

540 REFERENCES
541

542 Emmanuel Ameisen, Jack Lindsey, Adam Pearce, Wes Gurnee, Nicholas L. Turner, Brian Chen,
543 Craig Citro, David Abrahams, Shan Carter, Basil Hosmer, Jonathan Marcus, Michael Sklar,
544 Adly Templeton, Trenton Bricken, Callum McDougall, Hoagy Cunningham, Thomas Henighan,
545 Adam Jermyn, Andy Jones, Andrew Persic, Zhenyi Qi, T. Ben Thompson, Sam Zimmerman,
546 Kelley Rivoire, Thomas Conerly, Chris Olah, and Joshua Batson. Circuit tracing: Revealing
547 computational graphs in language models. *Transformer Circuits Thread*, 2025. URL
548 <https://transformer-circuits.pub/2025/attribution-graphs/methods.html>.
549

550 Stella Biderman, Hailey Schoelkopf, Quentin Anthony, Herbie Bradley, Kyle O'Brien, Eric Hal-
551 lahan, Mohammad Aflah Khan, Shivanshu Purohit, USVSN Sai Prashanth, Edward Raff, Aviya
552 Skowron, Lintang Sutawika, and Oskar van der Wal. Pythia: A suite for analyzing large language
553 models across training and scaling, 2023. URL <https://arxiv.org/abs/2304.01373>.
554

555 Steven Bills, Nick Cammarata, Dan Mossing, Henk Tillman, Leo Gao, Gabriel Goh, Ilya
556 Sutskever, Jan Leike, Jeff Wu, and William Saunders. Language models can explain neurons
557 in language models. <https://openaipublic.blob.core.windows.net/neuron-explainer/paper/index.html>, 2023.
558

559 Trenton Bricken, Adly Templeton, Joshua Batson, Brian Chen, Adam Jermyn, Tom Conerly, Nick
560 Turner, Cem Anil, Carson Denison, Amanda Askell, Robert Lasenby, Yifan Wu, Shauna Kravec,
561 Nicholas Schiefer, Tim Maxwell, Nicholas Joseph, Zac Hatfield-Dodds, Alex Tamkin, Karina
562 Nguyen, Brayden McLean, Josiah E. Burke, Tristan Hume, Shan Carter, Tom Henighan, and
563 Christopher Olah. Towards monosemanticity: Decomposing language models with dictionary
564 learning, 2023. URL <https://arxiv.org/abs/2312.11215>.
565

566 Bart Bussmann, Noa Nabeshima, Adam Karvonen, and Neel Nanda. Learning multi-level features
567 with matryoshka sparse autoencoders, 2025. URL <https://arxiv.org/abs/2503.17547>.
568

569 David Chanin, James Wilken-Smith, Tomáš Dulka, Hardik Bhatnagar, Satvik Golechha, and Joseph
570 Bloom. A is for absorption: Studying feature splitting and absorption in sparse autoencoders,
571 2024. URL <https://arxiv.org/abs/2409.14507>.
572

573 Dami Choi, Vincent Huang, Kevin Meng, Daniel D Johnson, Jacob Steinhardt, and
574 Sarah Schwettmann. Scaling automatic neuron description. <https://translue.org/neuron-descriptions>, October 2024.
575

576 Hoagy Cunningham, Aidan Ewart, Logan Riggs, Robert Huben, and Lee Sharkey. Sparse autoen-
577 coders find highly interpretable features in language models, 2023. URL <https://arxiv.org/abs/2309.08600>.
578

579 Jacob Dunefsky, Philippe Chlenski, and Neel Nanda. Transcoders find interpretable llm feature
580 circuits, 2024. URL <https://arxiv.org/abs/2406.11944>.
581

582 Esin Durmus, Alex Tamkin, Jack Clark, Jerry Wei, Jonathan Marcus, Joshua Batson, Kunal
583 Handa, Liane Lovitt, Meg Tong, Miles McCain, Oliver Rausch, Saffron Huang, Sam Bow-
584 man, Stuart Ritchie, Tom Henighan, and Deep Ganguli. Evaluating feature steering: A
585 case study in mitigating social biases, 2024. URL <https://anthropic.com/research/evaluating-feature-steering>.
586

587 Eoin Farrell, Yeu-Tong Lau, and Arthur Conmy. Applying sparse autoencoders to unlearn knowl-
588 edge in language models, 2024. URL <https://arxiv.org/abs/2410.19278>.
589

590 Javier Ferrando, Oscar Obeso, Senthooran Rajamanoharan, and Neel Nanda. Do i know this entity?
591 knowledge awareness and hallucinations in language models, 2025. URL <https://arxiv.org/abs/2411.14257>.
592

593 Leo Gao, Stella Biderman, Sid Black, Laurence Golding, Travis Hoppe, Charles Foster, Jason
594 Phang, Horace He, Anish Thite, Noa Nabeshima, Shawn Presser, and Connor Leahy. The pile:
595 An 800gb dataset of diverse text for language modeling, 2020. URL <https://arxiv.org/abs/2101.00027>.
596

594 Leo Gao, Tom Dupré la Tour, Henk Tillman, Gabriel Goh, Rajan Troll, Alec Radford, Ilya Sutskever,
 595 Jan Leike, and Jeffrey Wu. Scaling and evaluating sparse autoencoders, 2024. URL <https://arxiv.org/abs/2406.04093>.

597

598 Aaron Gokaslan, Vanya Cohen, Ellie Pavlick, and Stefanie Tellex. Openwebtext corpus. <http://Skylion007.github.io/OpenWebTextCorpus>, 2019.

600 Jing Huang, Atticus Geiger, Karel D’Oosterlinck, Zhengxuan Wu, and Christopher Potts. Rig-
 601 orously assessing natural language explanations of neurons, 2023. URL <https://arxiv.org/abs/2309.10312>.

603

604 Jing Huang, Zhengxuan Wu, Christopher Potts, Mor Geva, and Atticus Geiger. Ravel: Evaluating
 605 interpretability methods on disentangling language model representations, 2024. URL <https://arxiv.org/abs/2402.17700>.

607

608 Nick Jiang, Lily Sun, Lewis Smith, and Neel Nanda. Towards data-centric interpretability
 609 with sparse autoencoders, August 2025. URL <https://www.alignmentforum.org/posts/a4EDinzAYtRwpNmx9/towards-data-centric-interpretability-with-sparse>. Less-
 610 Wrong/Alignment Forum post.

611

612 Caden Juang, Gonçalo Paulo, Jacob Drori, and Nora Belrose. Open source automated interpretability
 613 for sparse autoencoder features, July 2024. URL <https://blog.eleuther.ai/autointerp/>.

614

615 Adam Karvonen, Benjamin Wright, Can Rager, Rico Angell, Jannik Brinkmann, Logan Smith,
 616 Claudio Mayrink Verdun, David Bau, and Samuel Marks. Measuring progress in dictionary
 617 learning for language model interpretability with board game models, 2024. URL <https://arxiv.org/abs/2408.00113>.

618

619 Adam Karvonen, Can Rager, Johnny Lin, Curt Tigges, Joseph Bloom, David Chanin, Yeu-Tong
 620 Lau, Eoin Farrell, Callum McDougall, Kola Ayonrinde, Demian Till, Matthew Wearden, Arthur
 621 Conmy, Samuel Marks, and Neel Nanda. Saebench: A comprehensive benchmark for sparse
 622 autoencoders in language model interpretability, 2025. URL <https://arxiv.org/abs/2503.09532>.

623

624 Laura Kopf, Philine Lou Bommer, Anna Hedström, Sebastian Lapuschkin, Marina M. C. Höhne, and
 625 Kirill Bykov. Cosy: Evaluating textual explanations of neurons, 2024. URL <https://arxiv.org/abs/2405.20331>.

626

627

628 Patrick Leask, Bart Bussmann, Michael Pearce, Joseph Bloom, Curt Tigges, Noura Al Moubayed,
 629 Lee Sharkey, and Neel Nanda. Sparse autoencoders do not find canonical units of analysis, 2025.
 630 URL <https://arxiv.org/abs/2502.04878>.

631

632 Tom Lieberum, Senthooran Rajamanoharan, Arthur Conmy, Lewis Smith, Nicolas Sonnerat, Vikrant
 633 Varma, János Kramár, Anca Dragan, Rohin Shah, and Neel Nanda. Gemma scope: Open sparse
 634 autoencoders everywhere all at once on gemma 2, 2024. URL <https://arxiv.org/abs/2408.05147>.

635

636 Jack Lindsey, Wes Gurnee, Emmanuel Ameisen, Brian Chen, Adam Pearce, Nicholas L. Turner,
 637 Craig Citro, David Abrahams, Shan Carter, Basil Hosmer, Jonathan Marcus, Michael Sklar, Adly
 638 Templeton, Trenton Bricken, Callum McDougall, Hoagy Cunningham, Thomas Henighan, Adam
 639 Jermyn, Andy Jones, Andrew Persic, Zhenyi Qi, T. Ben Thompson, Sam Zimmerman, Kelley
 640 Rivoire, Thomas Conerly, Chris Olah, and Joshua Batson. On the biology of a large language
 641 model. *Transformer Circuits Thread*, 2025. URL <https://transformer-circuits.pub/2025/attribution-graphs/biology.html>.

642

643 Aleksandar Makedov, George Lange, and Neel Nanda. Towards principled evaluations of sparse au-
 644 toencoders for interpretability and control, 2024. URL <https://arxiv.org/abs/2405.08366>.

645

646 Luke Marks, Alasdair Paren, David Krueger, and Fazl Barez. Enhancing neural network inter-
 647 pretability with feature-aligned sparse autoencoders, 2024. URL <https://arxiv.org/abs/2411.01220>.

648 Samuel Marks, Can Rager, Eric J. Michaud, Yonatan Belinkov, David Bau, and Aaron Mueller.
 649 Sparse feature circuits: Discovering and editing interpretable causal graphs in language models,
 650 2025a. URL <https://arxiv.org/abs/2403.19647>.

651 Samuel Marks, Johannes Treutlein, Trenton Bricken, Jack Lindsey, Jonathan Marcus, Siddharth
 652 Mishra-Sharma, Daniel Ziegler, Emmanuel Ameisen, Joshua Batson, Tim Belonax, Samuel R.
 653 Bowman, Shan Carter, Brian Chen, Hoagy Cunningham, Carson Denison, Florian Dietz, Satvik
 654 Golechha, Akbir Khan, Jan Kirchner, Jan Leike, Austin Meek, Kei Nishimura-Gasparian, Euan
 655 Ong, Christopher Olah, Adam Pearce, Fabien Roger, Jeanne Salle, Andy Shih, Meg Tong, Drake
 656 Thomas, Kelley Rivoire, Adam Jermyn, Monte MacDiarmid, Tom Henighan, and Evan Hubinger.
 657 Auditing language models for hidden objectives, 2025b. URL <https://arxiv.org/abs/2503.10965>.

658 Rajiv Movva, Kenny Peng, Nikhil Garg, Jon Kleinberg, and Emma Pierson. Sparse autoencoders
 659 for hypothesis generation, 2025. URL <https://arxiv.org/abs/2502.04382>.

660 Neel Nanda, Arthur Conmy, Lewis Smith, Senthooran Rajamanoharan, Tom Lieberum,
 661 János Kramár, and Vikrant Varma. Progress update #1 from the gdm mech inter-
 662 team, 2025. URL <https://www.alignmentforum.org/posts/HpAr8k74mW4ivCvCu/progress-update-from-the-gdm-mech-interp-team-summary>. LessWrong/Alignment Fo-
 663 rum post.

664 OpenAI, Josh Achiam, Steven Adler, Sandhini Agarwal, Lama Ahmad, Ilge Akkaya, Floren-
 665 cia Leoni Aleman, Diogo Almeida, Janko Altenschmidt, Sam Altman, Shyamal Anadkat, Red
 666 Avila, Igor Babuschkin, Suchir Balaji, Valerie Balcom, Paul Baltescu, Haiming Bao, Moham-
 667 mad Bavarian, Jeff Belgum, Irwan Bello, Jake Berdine, Gabriel Bernadett-Shapiro, Christopher
 668 Berner, Lenny Bogdonoff, Oleg Boiko, Madelaine Boyd, Anna-Luisa Brakman, Greg Brock-
 669 man, Tim Brooks, Miles Brundage, Kevin Button, Trevor Cai, Rosie Campbell, Andrew Cann,
 670 Brittany Carey, Chelsea Carlson, Rory Carmichael, Brooke Chan, Che Chang, Fotis Chantzis,
 671 Derek Chen, Sully Chen, Ruby Chen, Jason Chen, Mark Chen, Ben Chess, Chester Cho, Casey
 672 Chu, Hyung Won Chung, Dave Cummings, Jeremiah Currier, Yunxing Dai, Cory Decareaux,
 673 Thomas Degry, Noah Deutsch, Damien Deville, Arka Dhar, David Dohan, Steve Dowling, Sheila
 674 Dunning, Adrien Ecoffet, Atty Eleti, Tyna Eloundou, David Farhi, Liam Fedus, Niko Felix,
 675 Simón Posada Fishman, Juston Forte, Isabella Fulford, Leo Gao, Elie Georges, Christian Gib-
 676 son, Vik Goel, Tarun Gogineni, Gabriel Goh, Rapha Gontijo-Lopes, Jonathan Gordon, Morgan
 677 Grafstein, Scott Gray, Ryan Greene, Joshua Gross, Shixiang Shane Gu, Yufei Guo, Chris Hal-
 678 lacy, Jesse Han, Jeff Harris, Yuchen He, Mike Heaton, Johannes Heidecke, Chris Hesse, Alan
 679 Hickey, Wade Hickey, Peter Hoeschele, Brandon Houghton, Kenny Hsu, Shengli Hu, Xin Hu,
 680 Joost Huizinga, Shantanu Jain, Shawn Jain, Joanne Jang, Angela Jiang, Roger Jiang, Haozhun
 681 Jin, Denny Jin, Shino Jomoto, Billie Jonn, Heewoo Jun, Tomer Kaftan, Łukasz Kaiser, Ali Ka-
 682 mali, Ingmar Kanitscheider, Nitish Shirish Keskar, Tabarak Khan, Logan Kilpatrick, Jong Wook
 683 Kim, Christina Kim, Yongjik Kim, Jan Hendrik Kirchner, Jamie Kiros, Matt Knight, Daniel
 684 Kokotajlo, Łukasz Kondraciuk, Andrew Kondrich, Aris Konstantinidis, Kyle Kosic, Gretchen
 685 Krueger, Vishal Kuo, Michael Lampe, Ikai Lan, Teddy Lee, Jan Leike, Jade Leung, Daniel
 686 Levy, Chak Ming Li, Rachel Lim, Molly Lin, Stephanie Lin, Mateusz Litwin, Theresa Lopez,
 687 Ryan Lowe, Patricia Lue, Anna Makanju, Kim Malfacini, Sam Manning, Todor Markov, Yaniv
 688 Markovski, Bianca Martin, Katie Mayer, Andrew Mayne, Bob McGrew, Scott Mayer McKinney,
 689 Christine McLeavey, Paul McMillan, Jake McNeil, David Medina, Aalok Mehta, Jacob Menick,
 690 Luke Metz, Andrey Mishchenko, Pamela Mishkin, Vinnie Monaco, Evan Morikawa, Daniel
 691 Mossing, Tong Mu, Mira Murati, Oleg Murk, David Mély, Ashvin Nair, Reiichiro Nakano, Ra-
 692 jeev Nayak, Arvind Neelakantan, Richard Ngo, Hyeonwoo Noh, Long Ouyang, Cullen O’Keefe,
 693 Jakub Pachocki, Alex Paino, Joe Palermo, Ashley Pantuliano, Giambattista Parascandolo, Joel
 694 Parish, Emy Parparita, Alex Passos, Mikhail Pavlov, Andrew Peng, Adam Perelman, Filipe
 695 de Avila Belbute Peres, Michael Petrov, Henrique Ponde de Oliveira Pinto, Michael, Pokorny,
 696 Michelle Pokrass, Vitchyr H. Pong, Tolly Powell, Alethea Power, Boris Power, Elizabeth Proehl,
 697 Raul Puri, Alec Radford, Jack Rae, Aditya Ramesh, Cameron Raymond, Francis Real, Kendra
 698 Rimbach, Carl Ross, Bob Rotsted, Henri Roussez, Nick Ryder, Mario Saltarelli, Ted Sanders,
 699 Shibani Santurkar, Girish Sastry, Heather Schmidt, David Schnurr, John Schulman, Daniel Sel-
 700 sam, Kyla Sheppard, Toki Sherbakov, Jessica Shieh, Sarah Shoker, Pranav Shyam, Szymon Sidor,
 701 Eric Sigler, Maddie Simens, Jordan Sitkin, Katarina Slama, Ian Sohl, Benjamin Sokolowsky,

702 Yang Song, Natalie Staudacher, Felipe Petroski Such, Natalie Summers, Ilya Sutskever, Jie Tang,
 703 Nikolas Tezak, Madeleine B. Thompson, Phil Tillet, Amin Tootoonchian, Elizabeth Tseng, Pre-
 704 ston Tuggle, Nick Turley, Jerry Tworek, Juan Felipe Cerón Uribe, Andrea Vallone, Arun Vi-
 705 jayvergiya, Chelsea Voss, Carroll Wainwright, Justin Jay Wang, Alvin Wang, Ben Wang, Jonathan
 706 Ward, Jason Wei, CJ Weinmann, Akila Welihinda, Peter Welinder, Jiayi Weng, Lilian Weng,
 707 Matt Wiethoff, Dave Willner, Clemens Winter, Samuel Wolrich, Hannah Wong, Lauren Work-
 708 man, Sherwin Wu, Jeff Wu, Michael Wu, Kai Xiao, Tao Xu, Sarah Yoo, Kevin Yu, Qiming
 709 Yuan, Wojciech Zaremba, Rowan Zellers, Chong Zhang, Marvin Zhang, Shengjia Zhao, Tianhao
 710 Zheng, Juntang Zhuang, William Zhuk, and Barret Zoph. Gpt-4 technical report, 2024. URL
 711 <https://arxiv.org/abs/2303.08774>.

712 Gonçalo Paulo, Alex Mallen, Caden Juang, and Nora Belrose. Automatically interpreting millions
 713 of features in large language models, 2024. URL <https://arxiv.org/abs/2410.13928>.

714

715 Tamar Rott Shaham, Sarah Schwettmann, Franklin Wang, Achyuta Rajaram, Evan Hernandez, Jacob
 716 Andreas, and Antonio Torralba. A multimodal automated interpretability agent, 2025. URL
 717 <https://arxiv.org/abs/2404.14394>.

718 Chandan Singh, Aliyah R. Hsu, Richard Antonello, Shailee Jain, Alexander G. Huth, Bin Yu, and
 719 Jianfeng Gao. Explaining black box text modules in natural language with language models,
 720 2023. URL <https://arxiv.org/abs/2305.09863>.

721

722 Gemma Team, Morgane Riviere, Shreya Pathak, Pier Giuseppe Sessa, Cassidy Hardin, Surya Bhu-
 723 patiraju, Léonard Hussenot, Thomas Mesnard, Bobak Shahriari, Alexandre Ramé, Johan Fer-
 724 ret, Peter Liu, Pouya Tafti, Abe Friesen, Michelle Casbon, Sabela Ramos, Ravin Kumar, Char-
 725 line Le Lan, Sammy Jerome, Anton Tsitsulin, Nino Vieillard, Piotr Stanczyk, Sertan Girgin,
 726 Nikola Momchev, Matt Hoffman, Shantanu Thakoor, Jean-Bastien Grill, Behnam Neyshabur,
 727 Olivier Bachem, Alanna Walton, Aliaksei Severyn, Alicia Parrish, Aliya Ahmad, Allen Hutchi-
 728 son, Alvin Abdagic, Amanda Carl, Amy Shen, Andy Brock, Andy Coenen, Anthony Laforge,
 729 Antonia Paterson, Ben Bastian, Bilal Piot, Bo Wu, Brandon Royal, Charlie Chen, Chintu Kumar,
 730 Chris Perry, Chris Welty, Christopher A. Choquette-Choo, Danila Sinopalnikov, David Wein-
 731 berger, Dimple Vijaykumar, Dominika Rogozińska, Dustin Herbison, Elisa Bandy, Emma Wang,
 732 Eric Noland, Erica Moreira, Evan Senter, Evgenii Eltyshev, Francesco Visin, Gabriel Rasskin,
 733 Gary Wei, Glenn Cameron, Gus Martins, Hadi Hashemi, Hanna Klimczak-Plucińska, Harleen
 734 Batra, Harsh Dhand, Ivan Nardini, Jacinda Mein, Jack Zhou, James Svensson, Jeff Stanway, Jetha
 735 Chan, Jin Peng Zhou, Joana Carrasqueira, Joana Iljazi, Jocelyn Becker, Joe Fernandez, Joost van
 736 Amersfoort, Josh Gordon, Josh Lipschultz, Josh Newlan, Ju yeong Ji, Kareem Mohamed, Kar-
 737 tikeya Badola, Kat Black, Katie Millican, Keelin McDonell, Kelvin Nguyen, Kiranbir Sodhia,
 738 Kish Greene, Lars Lowe Sjoesund, Lauren Usui, Laurent Sifre, Lena Heuermann, Leticia Lago,
 739 Lilly McNealus, Livio Baldini Soares, Logan Kilpatrick, Lucas Dixon, Luciano Martins, Machel
 740 Reid, Manvinder Singh, Mark Iverson, Martin Görner, Mat Velloso, Mateo Wirth, Matt Davidow,
 741 Matt Miller, Matthew Rahtz, Matthew Watson, Meg Risdal, Mehran Kazemi, Michael Moynihan,
 742 Ming Zhang, Minsuk Kahng, Minwoo Park, Mofi Rahman, Mohit Khatwani, Natalie Dao,
 743 Nenshad Bardoliwalla, Nesh Devanathan, Neta Dumai, Nilay Chauhan, Oscar Wahltinez, Pankil
 744 Botarda, Parker Barnes, Paul Barham, Paul Michel, Pengchong Jin, Petko Georgiev, Phil Culliton,
 745 Pradeep Kuppala, Ramona Comanescu, Ramona Merhej, Reena Jana, Reza Ardeshir Rokni,
 746 Rishabh Agarwal, Ryan Mullins, Samaneh Saadat, Sara Mc Carthy, Sarah Cogan, Sarah Perrin,
 747 Sébastien M. R. Arnold, Sebastian Krause, Shengyang Dai, Shruti Garg, Shruti Sheth, Sue Ron-
 748 strom, Susan Chan, Timothy Jordan, Ting Yu, Tom Eccles, Tom Hennigan, Tomas Kociský, Tulsee
 749 Doshi, Vihan Jain, Vikas Yadav, Vilobh Meshram, Vishal Dharmadhikari, Warren Barkley, Wei
 750 Wei, Wenming Ye, Woohyun Han, Woosuk Kwon, Xiang Xu, Zhe Shen, Zhitao Gong, Zichuan
 751 Wei, Victor Cotruta, Phoebe Kirk, Anand Rao, Minh Giang, Ludovic Peran, Tris Warkentin, Eli
 752 Collins, Joelle Barral, Zoubin Ghahramani, Raia Hadsell, D. Sculley, Jeanine Banks, Anca Dra-
 753 gan, Slav Petrov, Oriol Vinyals, Jeff Dean, Demis Hassabis, Koray Kavukcuoglu, Clement Farabet,
 754 Elena Buchatskaya, Sebastian Borgeaud, Noah Fiedel, Armand Joulin, Kathleen Kenealy,
 755 Robert Dadashi, and Alek Andreev. Gemma 2: Improving open language models at a practical
 size, 2024. URL <https://arxiv.org/abs/2408.00118>.

756

757 Adly Templeton, Tom Conerly, Jonathan Marcus, Jack Lindsey, Trenton Bricken, Brian Chen, Adam
 758 Pearce, Craig Citro, Emmanuel Ameisen, Andy Jones, Hoagy Cunningham, Nicholas L Turner,

756 Callum McDougall, Monte MacDiarmid, C. Daniel Freeman, Theodore R. Sumers, Edward Rees,
757 Joshua Batson, Adam Jermyn, Shan Carter, Chris Olah, and Tom Henighan. Scaling monoseman-
758 ticity: Extracting interpretable features from claude 3 sonnet. *Transformer Circuits Thread*, 2024.
759 URL <https://transformer-circuits.pub/2024/scaling-monosemantics/index.html>.
760
761 Nicholas L Turner, Adam Jermyn, and Joshua Batson. Measuring feature sensitivity using dataset
762 filtering, July 2024. URL <https://transformer-circuits.pub/2024/july-update/index.html>.
763
764
765
766
767
768
769
770
771
772
773
774
775
776
777
778
779
780
781
782
783
784
785
786
787
788
789
790
791
792
793
794
795
796
797
798
799
800
801
802
803
804
805
806
807
808
809

810 A EVALUATION PROMPTS
811812 **System**
813

814
815 You are a meticulous AI researcher conducting an important investigation into a
816 specific feature inside a language model that activates in response to text
817 inputs. Your overall task is to generate additional text samples that cause the
818 feature to strongly activate.

819 You will receive a list of text examples on which the feature activates. Specific
820 tokens causing activation will appear between delimiters like {{this}}.
821 Consecutive activating tokens will also be accordingly delimited {{just like this
822 }}. If no tokens are highlighted with {}, then the feature does not activate on
823 any tokens in the input.

824 Note: features activate on a word-by-word basis. Also, feature activations can
825 only depend on words before the word it activates on.

826
827 **User**
828

829 Consider the feature that activates when the given examples below are present.
830 Your task is to generate text samples that strongly activate this feature. Study
831 the examples carefully to identify both their shared and varying traits. Your
832 generated samples should:

- 833 - Preserve any consistent traits, patterns, or constraints present across all
834 examples
- 835 - Match the diversity level shown in the examples---neither more diverse nor more
836 uniform
- 837 - Vary along the same dimensions that the examples vary (e.g., if examples differ
838 in tone but share a topic, maintain that pattern)
- 839 - Avoid introducing new types of variation not present in the example set
- 840 - Avoid collapsing into repetitive or overly similar outputs

841 Generate exactly 11 new samples separated by <SAMPLE_SEPARATOR/>. Note that the
842 feature may involve semantic content, grammatical structures, abstract concepts,
843 specific named entities (e.g., people, organizations, locations), or formatting
844 elements like newlines, punctuation, citations, or special characters, for
845 example, {{\n}}, or {{-}} represent newlines, {{,}} represents commas, {{-}}
846 represents hyphens, etc that are activating the feature. Present each sample
847 without numbering or bullets.

848 Important: place <SAMPLE_SEPARATOR/> between generated samples.

849 See the following 15 examples that activate the feature, separated by
850 <SAMPLE_SEPARATOR/>:

```
851 <SAMPLE_SEPARATOR/>
852 count();  

853 static const char*{{ resource}}{{_}}to_cstring(const char*{{ resource}}  

854  

855 <SAMPLE_SEPARATOR/>
```

856
857 What is the Java equivalent of JavaScript's{{ resource}} folder?↔↔My Wicket web
858 application contains

```
859 <SAMPLE_SEPARATOR/>
860 side-effect: since the check isn't so{{ resource}}↔intensive, you can set the  
861 time between checks  

862 ...
```

864

```

Assistant

866 "void free{{ resource}}Memory(void* ptr);
867 static const char* load_{{ resource}}Path(const char*{{ resource}});"
868
869 <SAMPLE_SEPARATOR/>
870
871 "How to configure the {{ resource}} directory in a Python Flask application?
872 I'm trying to serve static files from the"
873
874 <SAMPLE_SEPARATOR/>
875
876 warning: avoid heavy computation in the{{ resource}} allocation phase, it may
877 slow down startup.
878
879 <SAMPLE_SEPARATOR/>
880 ...
881
882
883
884
885

```

B FEATURE FILTERING DETAILS

We evaluated 112 SAEs from the SAEBench dataset and 29 from the GemmaScope dataset. The SAEBench set spans seven SAE families—BatchTopK, MatriyoshkaTopK, TopK, JumpReLU, ReLU, Gated, and PAnneal—whereas all GemmaScope SAEs are JumpReLU.

During the study, we observed that some activation texts distributed with SAEBench do not consistently activate their associated SAE features, likely due to truncation. To address this, we computed the *activation rate in truncated example text* for each feature, defined as the proportion of published activation texts that reliably elicit the feature. Features with an activation rate below 90% were excluded from our analysis. Table 1 and Table 2 reports the impact of this filtering on our study.

In Figure 9 we show our main Gemmascope results with different filtering thresholds. We see that for all choices of threshold, our main results hold.

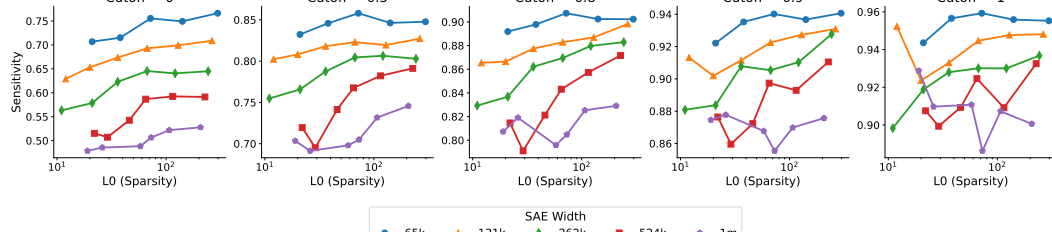


Figure 9: **Robustness to Feature Selection Cutoffs.** GemmaScope scaling results shown with different shortened text activation filter cutoffs. Our main results are robust to the choice of cutoff threshold, demonstrating that the observed scaling trends are not artifacts of our feature selection criteria.

Model	SAE Type	No. SAEs	Avg. No. Feat.	Avg. Sens.	90% Activation Rate Threshold			
					Avg. No. Remain.	Avg. Sens.	% Feat. Excluded	% Sens. Change
Gemma-2-2B	All, 16k	7	998	0.875	704	0.982	29.4%	12.2%
	All, 4k	7	999	0.918	801	0.984	19.8%	7.2%
	BatchTopK, 65k	6	969	0.814	562	0.980	42.1%	20.6%
	Gated, 65k	6	981	0.826	562	0.978	42.7%	18.4%
	JumpReLU, 65k	6	981	0.834	597	0.979	39.2%	17.4%
	MatryoshkaBatchTopK, 65k	6	964	0.776	485	0.979	49.7%	26.3%
	PAnneal, 65k	6	997	0.893	749	0.986	24.9%	10.7%
	Relu, 65k	6	994	0.848	646	0.983	35.0%	16.0%
Pythia-160M	TopK, 65k	6	972	0.820	574	0.979	41.0%	19.7%
	All, 16k	7	995	0.569	417	0.981	58.1%	137.8%
	All, 4k	7	1299	0.908	1029	0.986	21.0%	8.6%
	BatchTopK, 65k	6	978	0.850	674	0.987	30.9%	16.1%
	Gated, 65k	6	994	0.786	522	0.978	47.5%	24.6%
	JumpReLU, 65k	6	995	0.869	727	0.985	26.9%	13.4%
	MatryoshkaBatchTopK, 65k	6	968	0.817	624	0.986	35.1%	20.8%
	PAnneal, 65k	6	998	0.838	627	0.985	37.2%	17.6%
	Relu, 65k	6	997	0.834	633	0.984	36.5%	18.1%
	TopK, 65k	6	978	0.845	667	0.987	31.7%	17.3%
	ALL	112	1006	0.830	648	0.983	35.6%	18.4%

Table 1: SAE filtering statistics showing the impact of excluding features with activation rate below 90% in truncated example text. Columns show the model, SAE type, number of SAEs, average features per SAE before filtering, average sensitivity before filtering, and the effects after applying the 90% threshold: remaining features, new sensitivity, percentage excluded, and percentage sensitivity change.

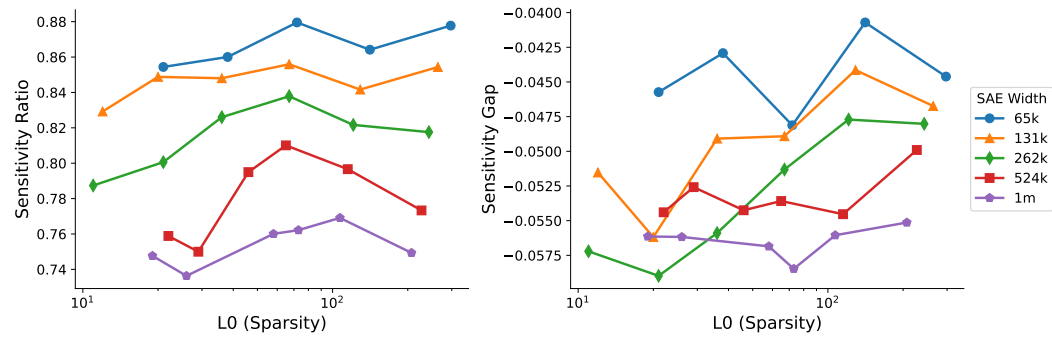
Width	No. SAEs	Features Evaluated	Features Remaining	% Excluded
65k	5	2336	1144	51.0%
131k	6	2438	990	59.4%
262k	6	2381	798	66.6%
524k	6	2339	629	73.2%
1M	6	2278	485	78.8%

Table 2: GemmaScope filtering statistics with 90% activation rate cutoff. All SAEs are JumpReLU trained on Gemma-2-2B layer 12 residual stream. Wider SAEs show increased feature exclusion rates.

972 **C NORMALIZED SENSITIVITY METRICS**
973

974 Our main analysis filters features based on their activation rate in truncated example text, excluding
975 35–79% of features with exclusion rates increasing for wider SAEs (Table 2). To further verify that
976 filtering does not explain our scaling results, we introduce two normalized metrics that account for
977 varying truncated activation rates without hard filtering.

978 Let p denote a feature’s activation rate on truncated example text and q denote its activation rate on
979 generated text. We define the **sensitivity ratio** as $\min(q/p, 1)$ (1 if $p = 0$), measuring what fraction
980 of a feature’s truncated-text activation rate is achieved on generated text. We define the **sensitivity**
981 **gap** as $\min(p - q, 0)$, measuring the drop in activation rate between truncated activating examples
982 and generated evaluation text.

983 Figure 10 shows both metrics averaged across GemmaScope SAE features. These metrics are com-
984 puted *without any feature filtering*. Wider SAEs show lower sensitivity ratios and larger sensitivity
985 gaps, reproducing our main finding that sensitivity declines with SAE width.

999 Figure 10: **Normalized sensitivity metrics across SAE widths.** Left: Sensitivity Ratio
1000 ($\min(q/p, 1)$) measures the fraction of a feature’s truncated activation ceiling achieved by generated
1001 text. Right: Sensitivity Gap ($\min(p - q, 0)$) measures the absolute difference between truncated and
1002 generated activation rates. Both metrics show that wider SAEs have lower sensitivity, confirming
1003 that our main finding is not an artifact of feature filtering.

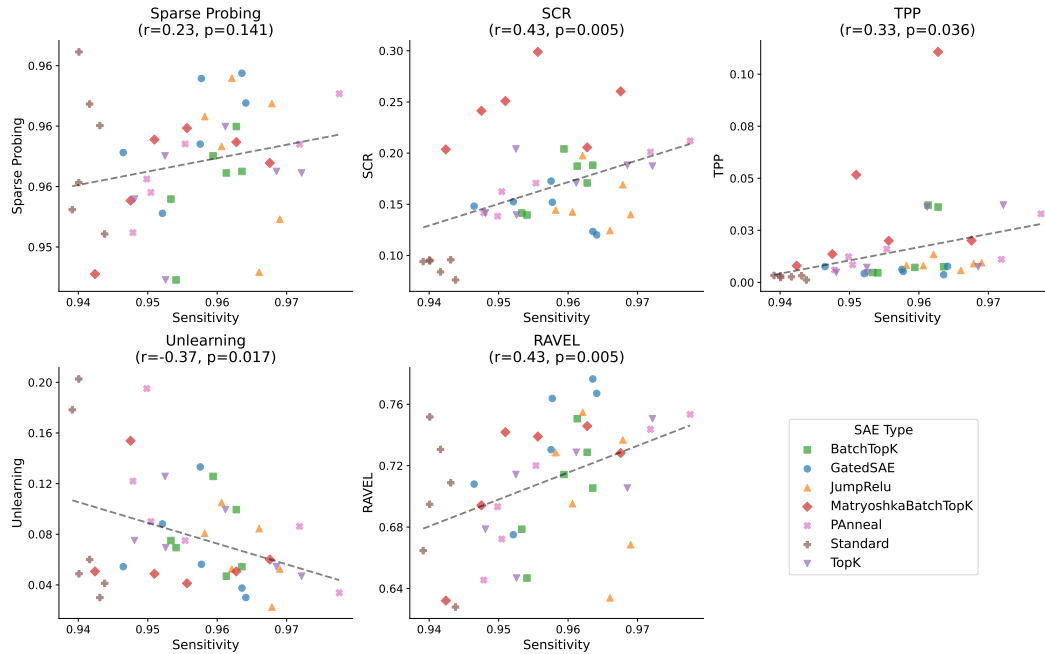
1004
1005
1006
1007
1008
1009
1010
1011
1012
1013
1014
1015
1016
1017
1018
1019
1020
1021
1022
1023
1024
1025

1026 D SENSITIVITY AND DOWNSTREAM TASK PERFORMANCE

1028 We conducted a preliminary analysis examining the relationship between sensitivity and downstream
 1029 task performance across 42 SAEs trained on Gemma-2-2B from SAEBench (Karvonen et al., 2025).
 1030 These SAEs span multiple architectures and sparsity levels.

1031 Figure 11 shows scatter plots of average SAE sensitivity against performance on five downstream
 1032 tasks. Sensitivity shows significant positive correlations with SCR ($r = 0.43, p = 0.005$), TPP
 1033 ($r = 0.33, p = 0.036$), and RAVEL ($r = 0.43, p = 0.005$), and a significant negative correlation
 1034 with Unlearning ($r = -0.37, p = 0.017$). The correlation with Sparse Probing was not significant
 1035 ($r = 0.23, p = 0.141$).

1036 We wish to emphasize that these results are exploratory and should be interpreted with caution. The
 1037 SAEs vary in architecture and sparsity, and we do not control for other SAE attributes (e.g., L0,
 1038 reconstruction quality) or correct for multiple comparisons. Future work could examine whether
 1039 sensitivity provides unique predictive value beyond existing metrics.



1062 **Figure 11: Sensitivity correlates with downstream task performance.** Scatter plots of average
 1063 SAE sensitivity against performance on five SAEBench tasks across 42 SAEs trained on Gemma-2-
 1064 2B. Sensitivity shows significant correlations with SCR, TPP, RAVEL, and Unlearning. Results are
 1065 exploratory; see text for caveats.

1080 E CONTROLLING FOR FEATURE FREQUENCY
1081
1082

1083 To ensure that our sensitivity results are not confounded by differences in feature frequency across
1084 SAE widths, we repeated our GemmaScope analysis with frequency-weighted sampling. Different
1085 width SAEs may have systematically different feature frequency distributions, which could poten-
1086 tially influence average sensitivity measurements.

1087
1088 E.1 WEIGHTING METHODOLOGY
1089

1090 We re-weighted features so that each SAE has the same effective frequency distribution. Specifically,
1091 for each SAE, we:

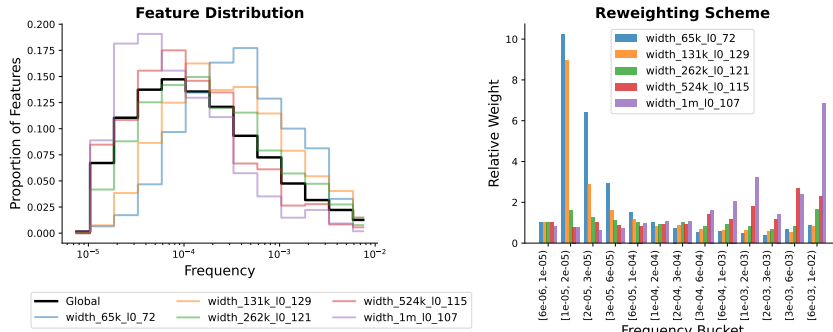
- 1094 1. Computed the frequency distribution of features across all SAEs in our study
1095
- 1096 2. Determined a target frequency distribution (the average distribution across all SAE widths)
1097
- 1098 3. Assigned weights to each feature inversely proportional to its frequency's representation in
1099 the SAE relative to the target distribution
1100
- 1101 4. Re-computed average sensitivity using these weights
1102

1104 Figure 12 illustrates this re-weighting process, showing how features at different frequencies are
1105 weighted to achieve a uniform distribution across SAEs.
1106

1107
1108 E.2 RESULTS WITH FREQUENCY CONTROL
1109

1111 Figure 13 shows the results after applying frequency weighting. Explicitly controlling for feature
1112 frequency via reweighting does not change our main results. Wider SAEs show lower average
1113 feature sensitivity. At a given width, SAEs with more active latents have higher sensitivity. This
1114 confirms that our main results are not an artifact of frequency distribution differences across SAE
1115 widths or sparsities.

1116 The similarity between these frequency-controlled results and our main findings (Figure 6) demon-
1117 strates that the sensitivity-width tradeoff is a robust phenomenon independent of feature frequency
1118 distributions.



1132 Figure 12: **Frequency re-weighting methodology.** Visualization of how features are re-weighted
1133 to control for frequency differences across SAE widths.

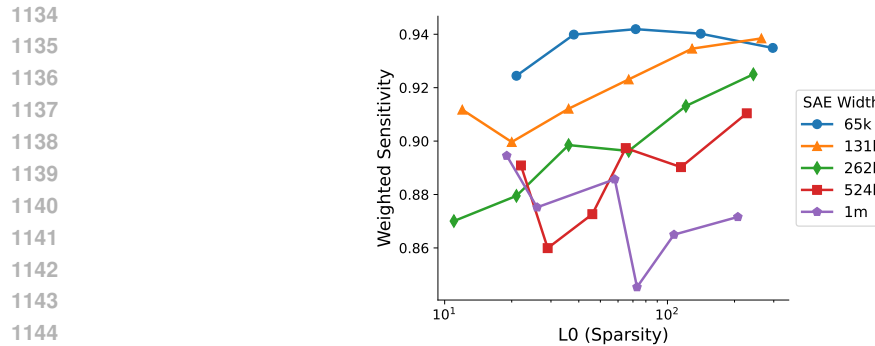


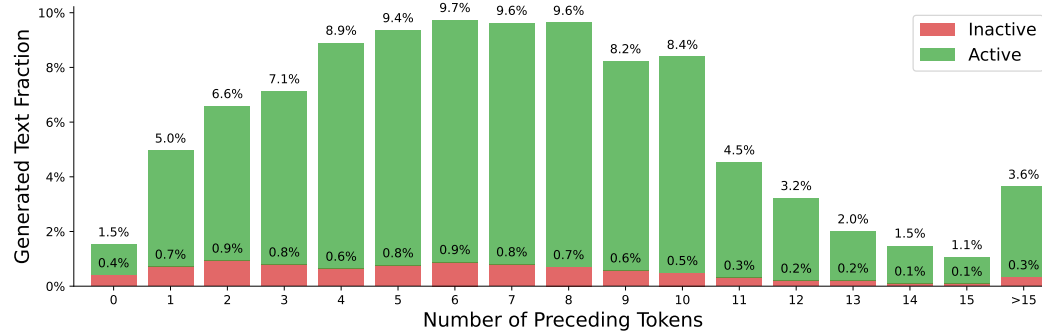
Figure 13: **Feature sensitivity with frequency weighting.** Average sensitivity across GemmaScope SAEs after re-weighting to control for feature frequency. The declining sensitivity with width persists, confirming our main findings.

1149
 1150
 1151
 1152
 1153
 1154
 1155
 1156
 1157
 1158
 1159
 1160
 1161
 1162
 1163
 1164
 1165
 1166
 1167
 1168
 1169
 1170
 1171
 1172
 1173
 1174
 1175
 1176
 1177
 1178
 1179
 1180
 1181
 1182
 1183
 1184
 1185
 1186
 1187

1188 F PRECEDING TOKEN LENGTH ANALYSIS
1189
1190
1191

1192 When we look through generated text that fails to activate the feature, we occasionally see cases
1193 where the text that intends to activate the feature appears very early in the sequence. We wanted to
1194 check if this early positioning of feature-related text was the cause of the feature failing to activate.
1195 To investigate this, we collected all generated texts and, for each one, looked for the first token that
1196 the model annotated with curly braces—this annotation indicates where the model was intending for
1197 the feature to activate, which we call target tokens. In Figure 14, we show the distribution of where
1198 the target token appears in the generated text.

1199 We found that generated texts indeed often have relatively short prefixes leading up to the target
1200 token. For example, in 1.5% of generations, the target token is actually the first token of the genera-
1201 tion, and in around 30% of generations, the target token is preceded by 5 or fewer tokens. However,
1202 we see that even in generated text samples where the target token occurs early in the sample, most
1203 of these samples successfully activate the feature. We do note that the proportion of generated text
1204 which fails to activate the feature is higher in generations with shorter prefixes. This represents a
1205 slight limitation of our evaluation that could be improved with better prompting and instructions,
1206 though the high success rate of feature activation even with short or no prefixes suggests that the
1207 bias does not significantly compromise our evaluation.



1223 **Figure 14: Target Token Position and Feature Activation Success.** For each generated text sam-
1224 ple, we identify the target token expected to activate the feature. The chart shows the number of
1225 tokens which occur in the generated text before the target token. Bars are colored based on whether
1226 the generated text successfully activated the feature (green) or failed to activate (red).

1235 G ADDITIONAL FEATURE EXAMPLES
1236
1237
1238

1239 We present additional feature dashboards showing interpretable features with zero sensitivity (Figure
1240 15), interpretable features with moderate sensitivity (Figure 16), and features with high sensitivity
1241 but low automated interpretability scores that appear qualitatively interpretable (Figure 17). Each
1242 dashboard displays 4 out of 15 activating text examples and 4 out of 10 generated text examples.

Figure 15: All 8 SAE features studied in Figure 3 that have sensitivity score 0 and auto-interp score over 0.9. For 3 of these features, low sensitivity may be due to generated passages immediately starting with the text intended to activate the feature.

1296	Feat ID: 563047 Desc: the concept of relationships or comparisons between different entities or conditions Freq: 2.74e-03 Sensitivity: 60.00% Interp Score: 92.86%
1297	Activating Text Examples Generated Text
1298	7.19 between a somatic mode of presentation on the one hand and a psychological mode on the 7.31 Data Handling*: Source files are segregated from the processing routines they drive. This
1299	10.06 . This finding suggests an interdependence of heavy alcohol consumption and psychological 0.00 a mixture of phospholipids blended to achieve a molar ratio of 100:20 cholesterol stabilized
1300	10.75 Data Separation**: Algorithmic code is separated from the data on which it operates. 0.00 examination highlights the synergistic effect of dopamine and glutamate receptor activity,
1301	10.94 not found when comparing a mixed level of parental education to a high level of parental 7.44 survival rate differences often show inverse correlations with tumor progression markers
1302	Feat ID: 297594 Desc: the word 'problems' and related concepts indicating issues or challenges Freq: 3.33e-05 Sensitivity: 60.00% Interp Score: 100.00%
1303	Activating Text Examples Generated Text
1304	8.75 of a trendy Melbourne art gallery, has her own problems – chasing down a delinquent 6.97 facing constant delays, she explained her problems quietly but with visible frustration at the
1305	7.34 to attempts at calibration. Of course, our problems are not likely to clear up so one may 0.00 discussing legislative issues, where the problems often are complex and intertwined with
1306	12.62 him, that's only the start of their problems. In this third Alex Caine book, sequel 8.12 Nina realized that understanding his problems required stepping into his perspective; that
1307	6.78 mnir becomes queen of a land with as many problems as the one she fled. Her long-lived 0.00 explaining the malfunction during the software demo, he hoped the technical problem would
1308	Feat ID: 2870 Desc: words related to teaching and education Freq: 2.57e-05 Sensitivity: 60.00% Interp Score: 92.86%
1309	Activating Text Examples Generated Text
1310	14.12 C.F.E. is an internationally respected teacher, trainer and clinician with an expertise in the 11.75 I always felt passionate about teaching because it allows me to inspire others. To teach is to
1311	11.00 you love about teaching? "I love to teach," Johnston said, "and the some of the 0.00 Kids bring so much energy and curiosity to the classroom. When I'm teaching, I get to see
1312	10.62 dots and monkeys." "What do you love about teaching? "I love to teach," Johnston 12.88 His work as a dedicated educator and community advocate has influenced many in the arts
1313	11.62 century. Architect, artist, furniture designer, and educator, Ralph Rapson has played a 0.00 Initially nervous about teaching, she grew into her role and now finds great joy in it. Her first
1314	Feat ID: 662898 Desc: theorems and corollaries referenced by their numbers in mathematical or academic contexts Freq: 6.25e-05 Sensitivity: 70.00% Interp Score: 92.86%
1315	Activating Text Examples Generated Text
1316	21.25 othe (2017). Theorem 3 includes existing DR moment functions as special cases where \$ 2.06 Consider Lemma 5 from Smith (2003) which establishes conditions for convergence in
1317	23.00 on this section can be applied. Corollary 3.2 from [@H] states that any Or 0.00 Based on Proposition 5 in the appendix, the asymptotic variance can be expressed as
1318	27.00 (\beta) and possibly additional functions. Proposition 2 of Newey (1994a) 0.00 From the proof of Lemma 5, we derive bounds on the estimator variance using
1319	11.44 font-variant:small-caps;">Theorem 3 *If the marginal distribution of * 2.44 The result of Corollary 3 follows immediately by applying the dominated convergence
1320	Feat ID: 267258 Desc: the variable placeholder 'i' in programming contexts Freq: 1.27e-04 Sensitivity: 50.00% Interp Score: 92.86%
1321	Activating Text Examples Generated Text
1322	8.50 CDATA_CTL); msg->buf[i] = (u8)(rxd 3.38 commandList[i].execute(); status = commandList[i].getStatus();
1323	15.50 rows <- createRow(sheet, rowIndex); for (j in 1: 0.00 <td *ngFor="let item of items; let i=index"> 18.88 ('model[0].h5.format(i)) end = time.time() 4.56 dataset['column_i'] = values[i]; 11.75 I2CDATA_CTL); msg[i + 1].buf[0] = (0.00 > </button>
1324	Feat ID: 898197 Desc: terms related to the concept of survival and its implications in various contexts Freq: 4.54e-05 Sensitivity: 70.00% Interp Score: 100.00%
1325	Activating Text Examples Generated Text
1326	10.00 three main purposes. The first was to facilitate the survival of the sponges across the 9.50 Examining the role of autophagy in prolonging cellular survival, we used markers for
1327	10.00 main purposes. The first was to facilitate the survival of the sponges across the battery of 0.00 Analysis of cohort data revealed a strong correlation between dietary intake and survival
1328	12.12 and size and the size of the grain affects its survivability in the archaeological 0.00 The clinical trial results showed higher median survival time among patients receiving
1329	15.50 Oxygen is a vital substrate to the continual function and survival of cerebral tissue. Rapid 15.38 Genetic diversity contributes significantly to the survival advantage seen in populations
1330	Feat ID: 362816 Desc: various expressions of the word "by" followed by different methods or approaches Freq: 2.67e-04 Sensitivity: 40.00% Interp Score: 92.86%
1331	Activating Text Examples Generated Text
1332	13.88 states, chose to achieve the same balance by alternate means. We have judges who 5.84 this result was obtained by innovative techniques involving machine learning and deep
1333	13.50 i=1;cdots, r\$; By a straightforward argument one may notice that the condition 0.00 the report was compiled by an experienced team of analysts specializing in market trends
1334	12.25 vertices. For each face choose a triangulation by non-intersecting diagonals. Let \$d\$ 0.00 the final decision was reached by mutual agreement among the stakeholders following
1335	10.88 so they will not be repeated here. By Order, the Court authorized the mailing of 0.00 marketing strategies improved by targeted campaigns using demographic and
1336	Feat ID: 878839 Desc: substrings containing specific sequences of letters within proper nouns and scientific terms Freq: 3.44e-04 Sensitivity: 50.00% Interp Score: 92.86%
1337	Activating Text Examples Generated Text
1338	7.66 --449--449--Ster ² \ [@CR22]\ (IMP2 0.00 font-style:italic;">Sergei V. Andreev and Tamara V.
1339	7.72 been used unfairly, please contact us<eos>Kralingse Zoom metro station<eos>Kralingse 5.53 been interrupted, please call the office<eos>Y ² lum metro station<eos>Y ² lum
1340	8.62 has been used unfairly, please contact us<eos>Kralingse Zoom metro station<eos>Kralingse 0.00 <eos> 4.53 ² B ² upl ² erum falcatum<root> 2.16 *Pleurotus ostreatus* (mushroom cap)
1341	
1342	
1343	
1344	
1345	
1346	
1347	Figure 16: 8 randomly sampled features from those studied in Figure 3 that have sensitivity score
1348	between 0.4 and 0.7 and high (≥ 0.9) auto-interp score.
1349	

Figure 17: 8 randomly sampled features from those studied in Figure 3 that have high (≥ 0.8) sensitivity score and low auto-interp score (≤ 0.6). These features tend to be interpretable despite their low automated interpretability score.